TransNav
http://www.transnav.eu
the International Journal
on Marine Navigation
and Safety of Sea Transportation
Volume 17
Number 1
March 2023
DOI: 10.12716/1001.17.01.21

# The Concept of Determining the Ship's Route Based on the Capability Plots

J. Wnorowski & A. Łebkowski
*Gdynia Maritime University, Gdynia, Poland*

ABSTRACT: Every year, new vessels equipped with dynamic positioning (DP) systems are built in shipyards around the world. Due to the increasing number of offshore vessels, a client hiring a vessel should analyse the vessel's positioning capability charts to determine which water areas the vessel is designed for. These charts are represented as polar diagrams. In the centre of the chart is a shape symbolising the ship's body, and the values on the chart represent the maximum wind speed that can affect the ship at a given angle, at which the vessel will maintain its position. Vessel capability charts can also be used by the crew during thrusters failures to determine at what angle to the wind direction the vessel should stand to minimise the impact of wind forces. Analyses that determine a vessel's ability to keep position can be performed by classification societies or other companies with approval from classification societies. The article presents the concept of a pathfinding algorithm to determines the route of the ship's passage with minimal energy consumption. The algorithm uses the information about environmental forces affecting the ship and information about thrust allocation obtained from Capability Plots

## 1 INTRODUCTION

Tracking a ship's position at sea has been one of the most important tasks of sailors since ancient times. Initially, sailors used natural clues such as the sun, stars and ocean currents to determine their position at sea. As science and technology advanced, sailing became more complicated, sailors began to use tools and technology that helped them more accurately determine their position at sea and plan their routes. In the 15th century, Portuguese sailors such as Bartolomeu Dias and Vasco da Gama took advantage of ocean winds and currents to cross the Indian Ocean. Between 1519 and 1522, Portuguese sailor Ferdinand Magellan made the first circumnavigation of the world, which became a milestone in the history of sailing and navigation. In the 19th century, British scientist and mathematician George Airy developed a system of geodetic triangulation that allowed sailors to accurately determine their position at sea using astronomical observations. In 1837, Airy published „Mathematical Tracts on the Lunar and Planetary Theories, the Figure of the Earth, Precession and Nutation, the Calculus of Variations, and the Undulatory Theory of Optics", where he described his system of geodetic triangulation. In 1960, the U.S. military's TRANSIT satellite system became the first satellite system to enable maritime navigation. In 1978, the US military introduced the Global Positioning System (GPS), which became a widely used navigation tool at sea and on land. With the development of computer technology and navigation software, routing a ship's passage has become increasingly automated. Modern navigation systems make it possible to quickly and accurately determine a route based on data on a ship's position, weather, currents and other factors affecting navigation [1–6].

An algorithm that can be used to determine the path of a ship's passage is the A* (A-star) algorithm. This is a graph search algorithm that is used to determine the shortest path between two vertices. In the case of ship passage routing, the A* algorithm can be used to find the shortest path, taking into account various constraints, such as the speed of the ship, obstacles in the way or sea currents. In publications [7–10], the authors presented an example application of the algorithm to determine the passage route of a ship taking into account changing weather conditions along the route. Another algorithm that works on a similar principle to A* is the D* (D-star) algorithm. The difference between the two is that the D* algorithm is used when the obstacles along the route are unknown, which means that the information provided to the algorithm must be updated. An example of the use of the D* algorithm is presented in the publication [11, 12], where the authors show how unmanned units can determine their own passage routes independently.

Another family of algorithms are those related to artificial intelligence. These include genetic algorithms, artificial neural networks and swarm algorithms [13–15]. A genetic algorithm is an optimization method that simulates the processes of population genetics. In the case of determining the passage route of a ship, this algorithm can be used to find the best route under complex conditions, taking into account a number of criteria, such as minimizing voyage time, minimizing costs, minimizing fuel consumption, etc. In the publication [16, 17], the authors present a way to determine a ship's passage route taking into consideration weather changes, other ships on the route and minimizing energy consumption. Swarm algorithms can also be used to optimize a ship's passage route, taking into account various external factors. These are metaheuristic optimization methods that mimic the behavior of flocks and swarms in nature. One of the more popular algorithms belonging to this type is an algorithm that mimics the behavior of ant colonies [18].

## 2 CAPABILITY PLOTS

In order to determine the ability of a DP-equipped vessel to keep a position under various environmental conditions, Capability Plots are made. These charts are presented in the form of polar diagrams. In the center of the chart is a symbol representing the shape of the vessel, while the values on the edge represent the angle of the environmental forces acting on the vessel. Figure 1 shows an example of this kind of chart:

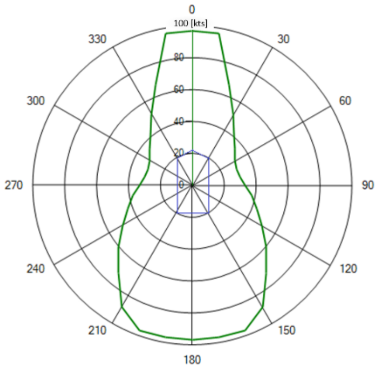


Figure 1. The example of Capability Plot

In the graph above, the green line indicates the maximum value of wind speed (in knots) that can act on the vessel at a given angle to make it keep its preset position. To counter the environmental forces, the vessel uses the thrusters it is equipped with.

In order to make the diagram in Figure 1, it is first necessary to develop a mathematical model of the environmental forces that affect the ship.

### 2.1 *Mathematical model of the environmental forces*

The mathematical model of environmental forces consists of the following components:
– Wind force affecting the vessel
– Sea current force affecting the vessel
– Sea waves force affecting the vessel

#### 2.1.1 *The wind force and torque*

In calculating the wind force on a vessel, it is assumed that the wind only affects the LPP/2 point of the vessel (LPP - Length Between Perpendiculars). By substituting the wind speed and wind angle into the following functions, the value of the wind force is obtained, acting on the X-axis and Y-axis of the vessel and the torque.

$$X_{wind} = q_w \cdot C_x\left(\alpha_w\right) \cdot A_{FW} \tag{1}$$

$$Y_{wind} = q_w \cdot C_Y\left(\alpha_w\right) \cdot A_{LW} \tag{2}$$

$$M_{wind} = q_w \cdot C_M\left(\alpha_w\right) \cdot A_{FW} \cdot H_{FW} \tag{3}$$

where: : $q_w$ – wind pressure on the ship's hull factor; $C_X$ – hull shape coefficient for X-axis; $\alpha_w$ – wind angle relative to LPP/2 point [$^0$]; $A_{FW}$ – frontal projected wind area [m$^2$]; $C_Y$ - hull shape coefficient for Y-axis; $A_{LW}$ – longitudinal projected wind area [m$^2$]; $C_M$ - hull shape coefficient for torque; $H_{FW}$ – longitudinal position of the area center of $A_{LW}$ [m]

The sea current force and torque

The force of the sea current and its torque are determined analogously to the wind force (equations 1-3). The difference between them is that in the case of wind force, the above-water part of the ship is taken into account, and in the case of the sea current, the underwater part:

$$X_{current} = q_c \cdot C_x\left(\alpha_C\right) \cdot A_{FC} \tag{4}$$

$$Y_{current} = q_c \cdot C_Y\left(\alpha_C\right) \cdot A_{LC} \tag{5}$$

$$M_{current} = q_c \cdot C_M\left(\alpha_C\right) \cdot A_{FC} \cdot H_{FC} \tag{6}$$

where: $q_c$ – sea current pressure on the ship's hull factor; $C_X$ – hull shape coefficient for X-axis; $\alpha_c$ – sea current angle relative to LPP/2 point[$^0$]; $A_{FC}$ – frontal projected sea current area [m$^2$]; $C_Y$ - hull shape coefficient for Y-axis; $A_{LC}$ – longitudinal projected submerged current area [m$^2$]; $C_M$ - hull shape coefficient for torque; $H_{FC}$ – longitudinal position of the area center of ALC [m]

Sea wave force and torque

The mathematical model of sea waves depends on the wave spectrum used. The most commonly used spectra are JONSWAP [19] and Pierson Moskowitz spectrum [20]. Classification society - DNV [21] recommends the use of the Moskowitz spectrum for analyses of a ship's ability to keep its position. The following is a mathematical model for determining the components of sea wave forces:

$$X_{wave} = q_c \cdot B \cdot h\left(dir_{temp}, bow_a, c_{WL}\right) \cdot f\left(T'_{surge}\right) \tag{7}$$

$$h\left(dir_{temp}, bow_a, C_{WL}\right) = 0.09 \cdot h_1\left(dir_{temp}, bow_a, C_{WL}\right) \cdot h_2\left(dir_{temp}\right) \tag{8}$$

$$h_{1A}\left(bow_a\right) = 0.8 \cdot bow_a^{45} \tag{9}$$

$$h_{1B}\left(C_{WL}\right) = 0.7 \cdot C_{WL}^2, C_{WL} \in \left[0.85, 1.15\right] \tag{10}$$

$$dir\left(dir_{temp}\right) = \begin{cases} dir_{temp}, 0 \le dir_{temp} \le \pi \\ 2\pi - dir_{temp}, \pi \le dir_{temp} \le 2\pi \end{cases} \tag{11}$$

$$h_1\left(dir_{temp}, bow_a, C_{WL}\right) = h_{1A}\left(bow_a\right) + \frac{dir\left(dir_{temp}\right)}{\pi}\left(h_{1B}\left(C_{WL}\right) - h_{1A}\left(bow_a\right)\right) \tag{12}$$

$$h_2\left(dir_{temp}\right) = 0.05 + 0.95 \cdot \tan^{-1}\left(1.45 \cdot \left(dir\left(dir_{temp}\right) - 1.75\right)\right) \tag{13}$$

$$f\left(T'\right) = \begin{cases} 1, & if\ T' < 1 \\ T'^{-3} \cdot e^{1-T'^{-3}}, & if\ T' \ge 1 \end{cases} \tag{14}$$

$$Y_{wave} = q_c \cdot L_{OS} \cdot \left(0.09 \cdot \sin\left(dir_{temp}\right)\right) \cdot f\left(T'_{sway}\right) \tag{15}$$

$$M_{wave} = Y_{wave} \cdot (X_{Los} + \left(0.05 - 0.14 \cdot \frac{dir\left(dir_{temp}\right)}{\pi}\right) \cdot L_{OS} \tag{16}$$

$$T'_{surge} = \frac{T_z}{0.9 \cdot L_{pp}^{0.33}} \tag{17}$$

$$T'_{sway} = \frac{T_z}{0.75 \cdot B^{0.5}} \tag{18}$$

$$H_s = 0.3125 \cdot V_w - 0.62 \tag{19}$$

$$T_z = 0.741 \cdot V_w + 0.536 \tag{20}$$

where: $B$ – maximum breadth at water line [m]; $bow_a$ – angle between the vessel x-axis and a line drawn foremost point in the water line to the point at y=B/4 on the water line [°]; $C_{WL}$ – water plane area coefficient; $dir_{temp}$ – waves coming from direction [°]; $L_{os}$ – longitudinal distance between the fore most and aft most point under water [m]; $X_{Los}$ – longitudinal position of Los/2 [m]; $L_{pp}$ – length between perpendiculars [m]; $H_s$ – significant wave height [m]; $V_w$ – wind speed [m/s]

To understand the relationship between mathematical formulas 7-20, it is necessary to read scientific description prepared by classification society DNV [21].

After determining the environmental forces that affect the ship, the next step is to find the distribution of thrust forces on the individual thrusters. The total value of the thrust force coming from all the propellers should balance external forces. To model the propellers, a standard from the classification society DNV can be used, marked as DNV-ST-0111.

## 3 DETERMINING THE ROUTE OF THE SHIP

Capability Plots are made to determine in which waters a ship can carry out positioning operations. When simulations are carried out, data are obtained on the effects of environmental forces on the ship and the distribution of thrust values to individual thrusters. This data can be used to develop the ship's passage route taking into account additional constraints, such as limiting energy consumption.

The first stage of defining the passage route is to specify the start and end points. Then divide the selected area into points with the chosen resolution. Figure 2 shows an example of dividing area into points with the start and end points marked.

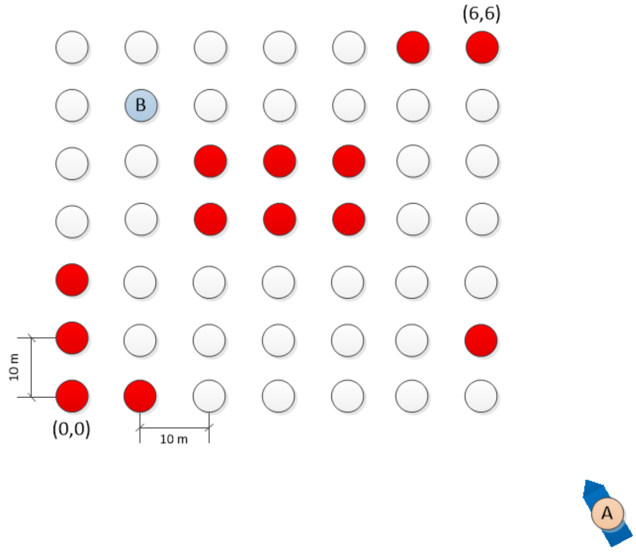

Figure 2. Example of division of the area into points with prohibited areas highlighted in red

After declaring the control point matrix, the capability plot for each point should be determined. Since a small range of area is taken into account, the environmental conditions at each point will be the same, making the capability plots the same as well.

After calculating the charts of the ship's ability to keep its position, it is necessary to determine the weights of the point-to-point transition. Since the environmental force acting on the ship depends on the angle of incidence of wind, sea current and waves on the hull, the transition weights can be determined according to the expected course at the next point. Knowing the maximum value of the environmental forces acting on the ship's hull, the weights can be normalized. Figure 3 shows an example of transition weights between points.

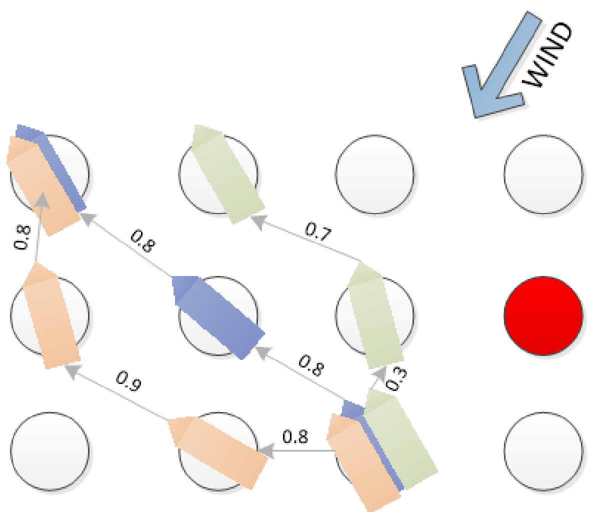

Figure 3. Weights of transitions between points depending on the route

Figure 3 shows the first three waypoints for 3 different ship routes Each route has different values of transition weights to the next point. They depend on the angle of incidence of the wind on the hull. From Figure 1, it can be seen that ships hold position most poorly when environmental forces act at about 90 degrees on the hull. This is because the lateral area is the largest, which translates into the greatest impact of environmental forces. For this reason, the weights in Figure 3 were determined as follows. The closer to the 90-degree angle the environmental forces act on the ship, the higher the weight.

Once the individual transition weights have been determined, it is necessary to find a route such that the transition values, when added together, come out as low as possible. In Figure 3 it can be seen that the green ship got the smallest sum, which translates into the fact that on a given route, environmental forces will affect the ship the least.

## 4 CONCLUSIONS

The article presents the concept of using Capability Plots to design a passage route between the starting and ending points. The algorithm uses information about the impact of environmental forces on the vessel's hull depending on the course and direction of wind, currents and wave action. Using the above information, the weights of transitions between successive waypoints can be determined. The route with the smallest sum of weights will be the most optimal in terms of the impact of environmental forces, which translates in theory into the lowest energy consumption.

The method presented in the article is based on graph search methods, so it can be used in conjunction with other algorithms such as A* when weather conditions are invariant. When weather conditions are variable, new graphs of the ability to keep a position at fixed time intervals must be calculated, so in this case the D* algorithm would be a better combination.

Currently, the algorithm for determining the thrust of individual thrusters uses an element of linear programming to find the minimum thrust defined by the constraint functions.

## REFERENCES

[1] A. Przybyłowski, "Sustainable Transport Planning & Development in the EU at the Example of the Polish Coastal Region Pomorskie," TRANSNAV-INTERNATIONAL JOURNAL ON MARINE NAVIGATION AND SAFETY OF SEA TRANSPORTATION, eISSN:2083-6481.

[2] A. Przybyłowski, "Sustainable urban mobility planning: Gdynia city case study," EiP, vol. 17, no. 2, p. 195, 2018, doi: 10.12775/EiP.2018.014.

[3] Z. Burciu, T. Abramowicz-Gerigk, W. Przybyl, I. Plebankiewicz, and A. Januszko, "The Impact of the Improved Search Object Detection on the SAR Action Success Probability in Maritime Transport," Sensors (Basel, Switzerland), vol. 20, no. 14, 2020.

[4] T. Abramowicz-Gerigk, Z. Burciu, and L. Hapke, "Innovative Project of Propellers and Thrusters Jet Loads during Ship Berthing Monitoring System," TransNav, vol. 13, no. 4, pp. 861–865, 2019, doi: 10.12716/1001.13.04.20.

[5] T. Abramowicz-Gerigk and Z. Burciu, "Design and Operational Innovations in Adapting the Existing Merchant River Fleet to Cost-Effective Shipping," Polish

Maritime Research, vol. 26, no. 4, pp. 157–164, 2019, doi: 10.2478/pomr-2019-0078.
[6] T. Abramowicz-Gerigk and Z. Burciu, "Application of Ship Motion Simulation in Reliability Assessment of Ship Entrance into the Port," TransNav, vol. 10, no. 4, pp. 613–617, 2016, doi: 10.12716/1001.10.04.10.
[7] K. S. Kula, "Automatic Control of Ship Motion Conducting Search in Open Waters," Polish Maritime Research, vol. 27, no. 4, pp. 157–169, 2020, doi: 10.2478/pomr-2020-0076.
[8] G. Chen, T. Wu, and Z. Zhou, "Research on Ship Meteorological Route Based on A-Star Algorithm," Mathematical Problems in Engineering, vol. 2021, pp. 1–8, 2021, doi: 10.1155/2021/9989731.
[9] Y. Liu, T. Wang, and H. Xu, "PE-A* Algorithm for Ship Route Planning Based on Field Theory," IEEE Access, vol. 10, pp. 36490–36504, 2022, doi: 10.1109/ACCESS.2022.3164422.
[10] K. Kula and M. Tomera, "Control System of Training Ship Keeping the Desired Path Consisting of Straight-lines and Circular Arcs," TransNav, vol. 11, no. 4, pp. 711–719, 2017, doi: 10.12716/1001.11.04.19.
[11] J. Yu et al., "Path planning of unmanned surface vessel in an unknown environment based on improved D*Lite algorithm," Ocean Engineering, vol. 266, p. 112873, 2022, doi: 10.1016/j.oceaneng.2022.112873.
[12] J. Zhang, H. Zhang, J. Liu, Da Wu, and C. G. Soares, "A Two-Stage Path Planning Algorithm Based on Rapid-Exploring Random Tree for Ships Navigating in Multi-Obstacle Water Areas Considering COLREGs," JMSE, vol. 10, no. 10, p. 1441, 2022, doi: 10.3390/jmse10101441.
[13] J. Lisowski, "Synthesis of a Path-Planning Algorithm for Autonomous Robots Moving in a Game Environment during Collision Avoidance," Electronics, vol. 10, no. 6, p. 675, 2021, doi: 10.3390/electronics10060675.
[14] J. Kruszewski and M. Mohamed-Seghir, "Concept of 'Sail by Wire' controller for a ship's propulsion system from an unmanned ship perspective," Journal of Marine Engineering & Technology, vol. 16, no. 4, pp. 185–192, 2017, doi: 10.1080/20464177.2017.1383340.
[15] J. Lisowski and M. Mohamed-Seghir, "Comparison of Computational Intelligence Methods Based on Fuzzy Sets and Game Theory in the Synthesis of Safe Ship Control Based on Information from a Radar ARPA System," Remote Sensing, vol. 11, no. 1, p. 82, 2019, doi: 10.3390/rs11010082.
[16] R. Saga, Z. Liang, N. Hara, and Y. Nihei, "Optimal Route Search Based on Multi-objective Genetic Algorithm for Maritime Navigation Vessels," in Lecture Notes in Computer Science, Human Interface and the Management of Information. Interacting with Information, S. Yamamoto and H. Mori, Eds., Cham: Springer International Publishing, 2020, pp. 506–518.
[17] K. Al-Hamad, M. Al-Ibrahim, and E. Al-Enezy, "A Genetic Algorithm for Ship Routing and Scheduling Problem with Time Window," AJOR, vol. 02, no. 03, pp. 417–429, 2012, doi: 10.4236/ajor.2012.23050.
[18] P.-F. Li, H.-B. Wang, and D.-Q. He, "Ship weather routing based on improved ant colony optimization algorithm," in 2018 IEEE Industrial Cyber-Physical Systems (ICPS), St. Petersburg, 2018, pp. 310–315.
[19] U.-J. Lee, W.-M. Jeong, and H.-Y. Cho, "Estimation and Analysis of JONSWAP Spectrum Parameter Using Observed Data around Korean Coast," JMSE, vol. 10, no. 5, p. 578, 2022, doi: 10.3390/jmse10050578.
[20] X. Chen et al., "Infrared Ocean Image Simulation Algorithm Based on Pierson–Moskowitz Spectrum and Bidirectional Reflectance Distribution Function," Photonics, vol. 9, no. 3, p. 166, 2022, doi: 10.3390/photonics9030166.
[21] Det Norske Veritas, DNV main page. [Online]. Available: https://www.dnv.com/ (accessed: Feb. 25 2023).